PAPER Special Section of Papers Selected from the 7th Digital Signal Processing Symposium

A Design Method for 3-Dimensional Band-Limiting FIR Filters Using McClellan Transformation

Toshiyuki YOSHIDA†, Akinori NISHIHARA† and Nobuo FUJII†, Members

SUMMARY In multidimensional signal sampling, the orthogonal sampling scheme is the simplest one and is employed in various applications, while a non-orthogonal sampling scheme is its alternative candidate. The latter sampling scheme is used mainly in application where the reduction of the sampling rate is important. In three-dimensional (3-D) signal processing, there are two typical sampling schemes which belong to the non-orthogonal samplings; one is face-centered cubic sampling (FCCS) and the other is body-centered cubic sampling (BCCS). This paper proposes a new design method for 3-D band-limiting FIR filters required for such non-orthogonal sampling schemes. The proposed method employs the McClellan transformation technique. Unlike the usual 3-D McClellan transformation, however, the proposed design method uses 2-D prototype filters and 2-D transformation filters to obtain 3-D FIR filters. First, 3-D general sampling theory is discussed and the two types of typical non-orthogonal sampling schemes, FCCS and BCCS, are explained. Then, the proposed design method of 3-D band-limiting filters for these sampling schemes is explained and an effective implementation of the designed filters is discussed briefly. Finally, design examples are given and the proposed method is compared with other method to show the effectiveness of our method.

key words: *digital signal processing, FIR filters, band-limiting filters, multidimensional filters, McClellan transformation*

1. Introduction

The uniform periodic sampling of 1-dimensional (1-D) signals is completely determined from the sampling period T, or its reciprocal $1/T$ known as the sampling density (sampling rate). In multidimensional cases, however, several sampling schemes exist with the identical sampling density, which is the most prominent difference between the 1-D and multidimensional cases [1], [2]. For example, in the 2-dimensional (2-D) case, the orthogonal and non-orthogonal sampling schemes are known, where the well-known "quincuncial sampling" [3] belongs to the latter type. By extending the quincuncial sampling scheme into 3-dimensional (3-D) space, face-centered cubic sampling (FCCS) and body-centered cubic sampling (BCCS) schemes [3], [4] are derived, which are explained intensively later in this paper. With these sampling schemes, it is possible to reduce the sampling rate of 3-D signals without limiting the maximum frequencies along the axes in the 3-D frequency domain. Applications of these sampling schemes can be found in Refs. [3]–[7], especially in the field of TV signal processing.

FCCS and BCCS can be obtained from orthogonally sampled 3-D signals by appropriate downsamplings. It is well-known that the downsampling process is preceded by a band limitation in frequency domain in order to avoid aliasing error [1]. Since the shapes of the baseband for FCCS and BCCS are generally very complicated, a design of such band-limiting 3-D filters becomes a difficult problem. A typical example of 3-D signals is a moving image. Therefore, FIR filters are suitable for 3-D band-limiting filters because completely linear-phase can be obtained, which is very important in image processing.

Many design methods have been proposed for multidimensional FIR filters, which are mainly classified into two categories: one is a direct design method using numerical optimizations such as linear programming (LP) [8], [9] and the other is a method employing frequency transformations like the McClellan transformation [10], [11]. The former method is capable to design almost optimal FIR filters for various specifications while it requires heavy calculation costs in general. For instance, consider a situation where we design a $15 \times 15 \times 15$-tap FIR filter by the LP method. The number of sampling points along with each frequency axis is assumed to be three times the number of taps. The design problem leads to an LP problem with 120 variables and about 40000 constraining equations, which requires roughly 40 Mbytes memory space for double precision arithmetic. It is practically difficult to solve such a huge problem even by mainframe computers due to the limitations of required memory space and computational time. On the other hand, the latter method drastically reduces the calculation cost. Furthermore, very efficient realization method has been proposed [12]. Since this method, however, restricts frequency responses to be realized, it is unsuitable in designing 3-D band-limiting filters for FCCS and BCCS.

Several design methods have been proposed for 3-D band-limiting filters [4]–[6]. This paper proposes a new design method of 3-D linear shift-invariant band-limiting FIR filters for FCCS and BCCS. The

Manuscript received December 25, 1992.
Manuscript revised April 6, 1993.
† The authors are with the Faculty of Engineering, Tokyo Institute of Technology, Tokyo, 152 Japan.

proposed design method uses 2-D transformation filters and 2-D prototype FIR filters to produce 3-D FIR filters [13]. The proposed method is a hybrid of the above mentioned two methods because 2-D prototype FIR filters are designed by a numerical optimization. The method has the following advantages, compared with the existing design techniques [4]-[6]:

1. The design is very easy, even if the filter order is very high.
2. A very efficient realization method exists for the designed filter.

It is also possible to use the designed filter as a recon struction filter for upsamping which restores the orthogonal sampling scheme from FCCS or BCCS.

The rest of this paper is organized as follows. In Sect. 2, we shall review the general 3-D sampling theory, and then the shapes of the baseband for FCCS and BCCS will be shown. In Sect. 3, the proposed design method will be described and an efficient realization method for the designed filters is discussed in Sect. 4. In Sect. 5, several design examples and comparisons with other design methods will be given. Finally, Sect. 6 concludes this paper.

2. 3-D Non-orthogonal Sampling and Band-Limiting Filters

2. 1 3-D Non-orthogonal Sampling

In this section, we first review the theory of multidimensional sampling for an arbitrary lattice [1], [2]. Then the properties of FCCS and BCCS [3], [4] are explained to show the ideal frequency responses of band-limiting filters for FCCS and BCCS.

An N-dimensional (N-D) lattice Λ is defined as the set of all integer combination of N independent basis vectors $\boldsymbol{v}_1, \boldsymbol{v}_2, \cdots, \boldsymbol{v}_N$ in N-D space R^N [2],

$$\Lambda=\{\boldsymbol{n} \mid n=V\boldsymbol{k},\ \boldsymbol{k}\in Z^N\}, \tag{1}$$

where V is a matrix defined as

$$V=[\boldsymbol{v}_1|\boldsymbol{v}_2|\cdots|\boldsymbol{v}_N], \tag{2}$$

and $\boldsymbol{n}$ and $\boldsymbol{k}$ are integer vectors in Z^N.

The sampling points in an N-D uniform periodic sampling scheme consist an N-D lattice Λ, which is completely represented by the corresponding matrix V referred as "sampling matrix." Since a sampling matrix V is composed of linearly independent vectors as in Eq. (2), det V is always nonzero and $1/|\det V|$ represents the sampling density (sampling rate). A given sampling matrix V uniquely determines the sampling scheme, while generally, the converse is not true; if V is the sampling matrix for a sampling scheme, then EV is also the sampling matrix, where E is an integer matrix with det $E=\pm 1$.

Among various types of uniform periodic samplings, the simplest and most common sampling scheme is an orthogonal sampling whose sampling points consist a simple cubic lattice. Such a sampling is referred as "simple cubic sampling (SCS)" in this paper, one of whose sampling matrices is written as

$$V_{SCS}=[\boldsymbol{v}_1|\boldsymbol{v}_2|\boldsymbol{v}_3]=\begin{bmatrix} x_1 & 0 & 0 \\ 0 & x_2 & 0 \\ 0 & 0 & x_3 \end{bmatrix}, \tag{3}$$

where x_1, x_2 and x_3 are the sampling periods with respect to the axes n_1, n_2 and n_3, respectively. Figure 1 (a) shows the arrangement of sampling points of SCS, where $x_1=x_2=x_3=1$ is assumed. This condition will be assumed throughout this paper.

In 3-D sampling, two typical sampling schemes other than SCS are known which belong to the non-orthogonal sampling. One is "face-centered cubic sampling (FCCS)" and the other is "body-centered cubic sampling (BCCS)," whose sampling points consist a face-centered cubic lattice and a body-centered cubic lattice, respectively.

Figure 2 (a) illustrates the arrangement of sampling points of FCCS and its basis vectors, which

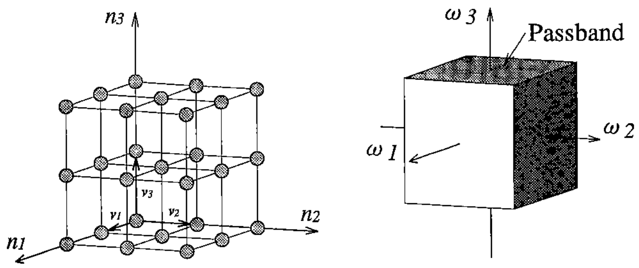

(a) (b)

Fig. 1 Simple cubic sampling scheme. (a) Arrangement of sampling points in spatio-temporal domain and the basis vectors. (b) First Brillouin zone in frequency domain.

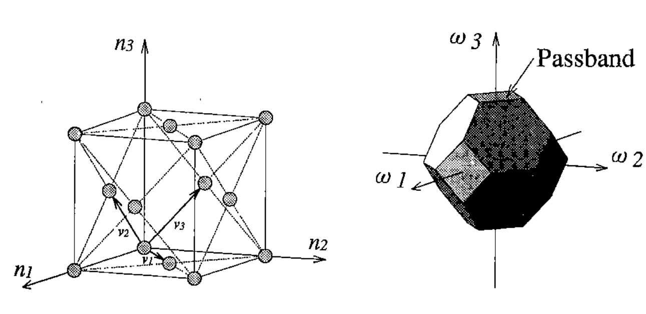

(a) (b)

Fig. 2 Face-centered cubic sampling scheme. (a) Arrangement of sampling points in spatio-temporal domain and the basis vectors. (b) First Brillouin zone in frequency domain.

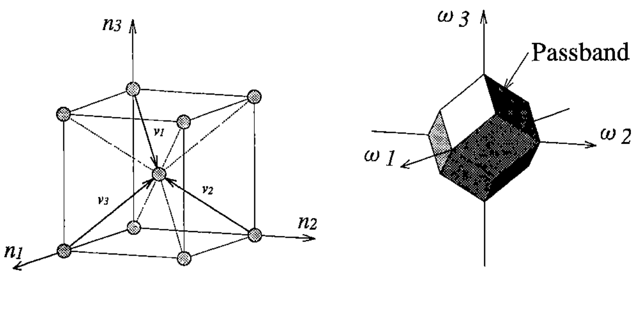

(a) (b)

Fig. 3 Body-centered cubic sampling scheme. (a) Arrangement of sampling points in spatio-temporal domain and the basis vectors. (b) First Brillouin zone in frequency domain.

defines the sampling matrix

$$V_{FCCS}=\begin{bmatrix}1 & 1 & 0\\ 1 & 0 & 1\\ 0 & 1 & 1\end{bmatrix}. \tag{4}$$

Similarly, Fig. 3 (a) illustrates BCCS together with its basis vectors, from which the sampling matrix

$$V_{BCCS}=\begin{bmatrix}1 & 1 & -1\\ 1 & -1 & 1\\ -1 & 1 & 1\end{bmatrix}. \tag{5}$$

is derived. These figures show that a suitable downsampling of SCS yields FCCS and BCCS structures. Since $|\det V_{SCS}|=1$, $|\det V_{FCCS}|=2$ and $|\det V_{BCCS}|=4$ are obtained from Eqs. (3)-(5), it follows that the sampling densities of FCCS and BCCS are 1/2 and 1/4 of that of SCS, respectively.

2.2 Alias-Free Baseband Shapes for FCCS and BCCS

Since a downsampling in spatio-temporal domain reduces the volume of the baseband in frequency domain, aliasing error is introduced into the signal spectrum. To avoid such aliasing error, a suitable band limitation precedes the downsampling.

Let $x_V(\boldsymbol{k})$ be a sampled signal with a sampling matrix V and $X_V(\boldsymbol{\omega})$ ($\boldsymbol{\omega}=[\omega_1\omega_2\omega_3]^t$) be its Fourier transform, then these are related as

$$X_V(\boldsymbol{\omega})=\iiint x_V(\boldsymbol{k})\exp(-j\boldsymbol{\omega}^t V\boldsymbol{k})\,d\boldsymbol{k}. \tag{6}$$

Consider a new matrix defined as

$$U=V^{-t}, \tag{7}$$

where $\{\cdot\}^{-t}$ denotes the inverse and transpose of a matrix. Because of the relation

$$X_V(\boldsymbol{\omega})=X_V(\boldsymbol{\omega}+2\pi U\boldsymbol{l}) \quad (\boldsymbol{l}\in Z^3), \tag{8}$$

the matrix U represents the periodicity of the Fourier spectrum $X_V(\boldsymbol{\omega})$ and is called the "aliasing matrix." From Eqs. (4), (5) and (7), the aliasing matrices for FCCS and BCCS are calculated as

$$U_{FCCS}=V_{FCCS}^{-t}=\begin{bmatrix}1/2 & 1/2 & -1/2\\ 1/2 & -1/2 & 1/2\\ -1/2 & 1/2 & 1/2\end{bmatrix} \tag{9}$$

and

$$U_{BCCS}=V_{BCCS}^{-t}=\begin{bmatrix}1/2 & 1/2 & 0\\ 1/2 & 0 & 1/2\\ 0 & 1/2 & 1/2\end{bmatrix}, \tag{10}$$

respectively.

According to the periodicity, the Fourier spectrum should be band-limited prior to the downsampling not to introduce aliasing error. For a given periodicity of the Fourier spectrum, i.e. the aliasing matrix U, an infinite number of alias-free baseband shapes exist. Among various types of such baseband shapes, one of the most important baseband shapes is the "first Brillouin zone" formed by the intersection of planes which are perpendicularly bisecting the lines joining one center point to its nearest neighbors [3], [4]. The first Brillouin zones for SCS, FCCS and BCCS are illustrated in Figs. 1(b), 2 (b) and 3 (b), respectively.

The limitation of the spectrum into the first Brillouin zone requires a 3-D band-limiting filter whose passband corresponds to the interior of the zone. The next section discusses a design method of 3-D band-limiting filters for FCCS and BCCS.

3. Design of 3-D Band-Limiting Filters for FCCS and BCCS

3.1 Design of 3-D FIR Filters with McClellan Transformations

The frequency response of a zero-phase FIR filter is written in the form

$$H_1(e^{j\omega})=\sum a_n \cos n\omega, \tag{11}$$

where a_n's are constants determined from the impulse response of the filter. Using the Chebyshev polynomials, Eq. (11) can be converted into a polynomial of $\cos\omega$,

$$H_1(e^{j\omega})=\sum a_n T_n(\cos\omega). \tag{12}$$

A 3-D McClellan transformation replaces $\cos\omega$ in Eq. (12) with a zero-phase 3-D transformation filter $F(e^{j\omega_1}, e^{j\omega_2}, e^{j\omega_3})$;

$$H_3(e^{j\omega_1}, e^{j\omega_2}, e^{j\omega_3})=\sum a_n T_n(F(e^{j\omega_1}, e^{j\omega_2}, e^{j\omega_3})), \tag{13}$$

which produces a 3-D FIR filter $H_3(e^{j\omega_1}, e^{j\omega_2}, e^{j\omega_3})$. By appropriately selecting filter coefficients, several types of FIR filters, e.g. spherically symmetric filters, can be designed with $3\times3\times3$ transformation filters. For more complex 3-D filters, however, higher-order transformations are required because the freedom of design in $3\times3\times3$ transformations is very low. Instead of using higher-order 3-D transformation filters, this paper uses 2-D prototype FIR filters and 2-D 3×3-tap transformation filters [13] to design 3-D band-limiting filters shown in Figs. 2 (b) and 3 (b).

Let $H_3(e^{j\omega_1}, e^{j\omega_2}, e^{j\omega_3})$ be the frequency response to be designed and $F(e^{j\omega_1}, e^{j\omega_2})$ be a transformation. Furthermore, let $H_2(e^{j\omega_1}, e^{j\omega_2})$ be the 2-D cross-sectional frequency responses of H_3 with respect to the axis ω_3 as

$$H_2(e^{j\omega_1}, e^{j\omega_2}) = H_3(e^{j\omega_1}, e^{j\omega_2}, e^{j\omega_3})|_{\omega_3=\omega_0}. \tag{14}$$

Now consider the following condition;

All the 2-D frequency responses in Eq. (14) for $-\pi \leqq \omega_0 \leqq \pi$ can be designed with the identical trasformation $F(e^{j\omega_1}, e^{j\omega_2})$ and 1-D prototype filters $H_1^{\omega'}(e^{j\omega})$ (The notation $H_1^{\omega'}(e^{j\omega})$ represents a 1-D filter with the cutoff frequency ω').

If the frequency response $H_3(e^{j\omega_1}, e^{j\omega_2}, e^{j\omega_3})$ satisfies this condition, it is possible to design it in the following manner. First, we design the 2-D zero-phase prototype FIR filter $H_2(e^{j\omega_a}, e^{j\omega_b})$ whose passband (PB) and stopband (SB) are given as

$$\mathrm{PB} = \{(\omega_a, \omega_b) \,||\omega_a| \in \{\text{PB of } H_1^{|\omega_b|}(e^{j\omega})\}, \quad 0 \leqq |\omega_a|, |\omega_b| \leqq \pi\} \tag{15}$$

and

$$\mathrm{SB} = \{(\omega_a, \omega_b) \,||\omega_a| \in \{\text{SB of } H_1^{|\omega_b|}(e^{j\omega})\}, \quad 0 \leqq |\omega_a|, |\omega_b| \leqq \pi\}, \tag{16}$$

respectively. Second, we replace the function $\cos\omega_a$ with the transformation filter F, and the frequency ω_b with ω_3;

$$\begin{cases} \cos\omega_a = F(e^{j\omega_1}, e^{j\omega_2}) \\ \omega_b = \omega_3. \end{cases} \tag{17}$$

Then the obtained filter is an approximation of the desired frequency response.

Assume that the designed 2-D prototype is a $(2N_a+1) \times (2N_b+1)$-tap quadrantally-symmetric zero-phase FIR filter, and that the transformation filter is 3×3-tap zero-phase FIR filter. The transfer function of the 2-D prototype is given by

$$H_2(z_a, z_b) = \sum_{i=-N_a}^{N_a} \sum_{j=-N_b}^{N_b} h_{ij} z_a^{-i} z_b^{-j}, \tag{18}$$

where $z_a = e^{j\omega_a}$ and $z_b = e^{j\omega_b}$ on the unit circle, and h_{ij}'s represent the impulse response of the 2-D prototype with $h_{ij} = h_{|i||j|}$. Using the Chebyshev polynomials, the frequency response in Eq. (18) can be expressed as

$$H_2(e^{j\omega_a}, e^{j\omega_b}) = \sum_{i=0}^{N_a} \sum_{j=0}^{N_b} a_{ij} T_i(\cos\omega_a) \cos j\omega_b, \tag{19}$$

where a_{ij}'s are constants determined from the impulse response. According to the above design method, the transfer function of the resultant 3-D filter is written as

$$H_3(z_1, z_2, z_3) = \sum_{i=0}^{N_a} \sum_{j=-N_b}^{N_b} b_{ij} T_i(F(z_1, z_2)) z_3^{-j}, \tag{20}$$

where b_{ij}'s are again constants derived from a_{ij}'s.

3.2 Design of 3-D Band-Limiting Filters for FCCS

3.2.1 Proposed Design Method

Here we consider a design method of band-limiting filters for FCCS, whose passband (desired value=1) and stopband (desired value=0) are the interior and the exterior of the first Brillouin zone shown in Fig. 2

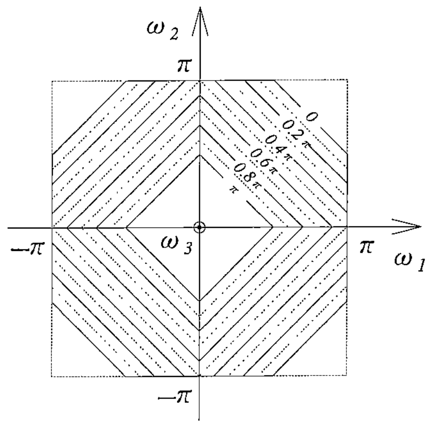

Fig. 4 Cross-sectional frequency response of band-limiting filters for FCCS with ω_3=constant. The values represent the intersections with the axis ω_3.

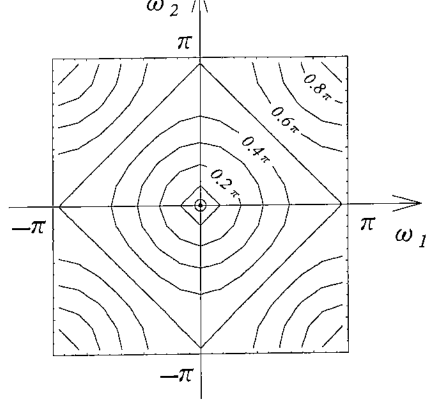

Fig. 5 Equiamplitude lines of the transformation (21) with respect to the parameters ω_a.

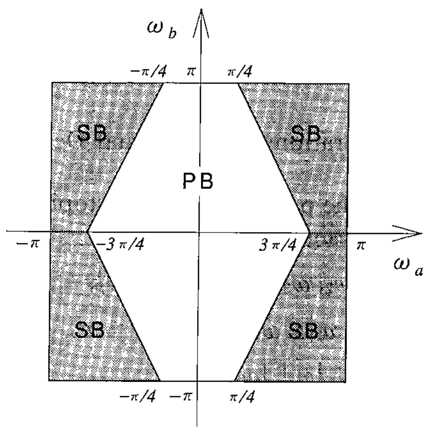

Fig. 6 2-D prototype FIR filter required for FCCS.

(b), respectively.

Figure 4 shows the cross-sectional frequency response with $\omega_3=\omega_0=$const. in ω_1-ω_2 plane. On the other hand, Fig. 5 shows the equiamplitude lines of a transformation [10]

$$\begin{cases} F(z_1, z_2)=\dfrac{z_1+z_1^{-1}+z_2+z_2^{-1}}{4} \\ F(e^{j\omega_1}, e^{j\omega_2})=\dfrac{\cos\omega_1+\cos\omega_2}{2}\equiv\cos\omega_a \end{cases} \tag{21}$$

with respect to the parameter ω_a. Note that all of the cross-sectional frequency responses in Fig. 4 can be approximated by the trasformation (21) and suitable 1-D prototypes, which satisfies the condition in the previous section. A comparison of the diagonal responses in Figs. 4 and 5 requires the filter shown in Fig. 6 as the 2-D prototype $H_2(e^{j\omega_a}, e^{j\omega_b})$. Therefore, a design of the 2-D prototype in Fig. 6 and an application of the transformation (21) complete the design of the desired band-limiting filter for FCCS.

3. 2. 2 Considerations on an Actual Design

In an actual filter design, a transition band should exists between the passband and the stopband. Here we assume that the passband and the stopband of the 3-D filter to be designed are given as

$$\mathrm{PB}=\{(\omega_1, \omega_2, \omega_3)\,||\omega_1|+|\omega_2|+|\omega_3|\leqq\omega_p^3,\ 0\leqq|\omega_1|, |\omega_2|, |\omega_3|\leqq\pi\} \tag{22}$$

$$\mathrm{SB}=\{(\omega_1, \omega_2, \omega_3)\,||\omega_1|+|\omega_2|+|\omega_3|\geqq\omega_s^3,\ 0\leqq|\omega_1|, |\omega_2|, |\omega_3|\leqq\pi\}, \tag{23}$$

respectively (Note that the superscripts represent the dimensionality of the filter.) Similarly for the 2-D prototype shown in Fig. 6, the passband and stopband are defined as

$$\mathrm{PB}=\{(\omega_a, \omega_b)\,|\,2|\omega_a|+|\omega_b|\leqq\omega_p^2,\ 0\leqq|\omega_a|, |\omega_b|\leqq\pi\} \tag{24}$$

$$\mathrm{SB}=\{(\omega_a, \omega_b)\,|\,2|\omega_a|+|\omega_b|\geqq\omega_s^2,\ 0\leqq|\omega_a|, |\omega_b|\leqq\pi\}, \tag{25}$$

respectively. The positive parameters ω_p^3, ω_s^3, ω_p^2 and ω_s^2 give the band-edge frequencies for 3-D band-limiting filters and 2-D prototype filters, respectively

By substituting the passband of the 2-D prototype $|\omega_a|\leqq(\omega_p^2-|\omega_3|)/2$ for a given $\omega_b=\omega_3$ into Eq. (21),

$$|\omega_3|\geqq\omega_p^2-2\cos^{-1}\left(\frac{\cos\omega_1+\cos\omega_2}{2}\right) \tag{26}$$

is obtained, and a substitution of Eq. (26) into Eq. (22) leads to a relation

$$\omega_p^2-\omega_p^3\geqq 2\cos^{-1}\left(\frac{\cos\omega_1+\cos\omega_2}{2}\right)-|\omega_1|-|\omega_2|. \tag{27}$$

Since the maximum value of the right hand side is 0.1755π in the range $0\leqq|\omega_1|, |\omega_2|\leqq\pi$,

$$\omega_p^2\geqq\omega_p^3+0.1755\pi \tag{28}$$

is obtained and in a similar way,

$$\omega_s^2\leqq\omega_s^3-0.1755\pi \tag{29}$$

is also derived, from which the band-edge frequencies of the 2-D prototype can be determined for the given parameters ω_p^3 and ω_s^3 in Eqs. (22) and (23). Note that the passband and the stopband deviations of the 3-D band-limiting filter coincide with those of its 2-D prototype, respectively.

3. 3 Design of 3-D Band-Limiting Filters for BCCS

3. 3. 1 Proposed Design Method

The ideal filter characteristics to be approximated is shown in Fig. 3(b). Figure 7 shows its cross-sectional frequency response with $\omega_3=\omega_0=$const. in $\omega_1-\omega_2$ plane. If we rotate the $\omega_1-\omega_2$ frequency plane with a transformation

$$\begin{bmatrix}\omega_1' \\ \omega_2'\end{bmatrix}=\begin{bmatrix}1 & -1 \\ 1 & 1\end{bmatrix}\begin{bmatrix}\omega_1 \\ \omega_2\end{bmatrix} \tag{30}$$

by 45°, it follows that the resultant frequency response in ω_1' and ω_2' can be realized by applying the transform (21) to a 2-D diamond-shaped prototype shown in Fig. 8. Therefore, the inverse transform of Eq. (30) realizes the desired frequency response in Fig. 7 except that the areas A, B, C and D become passbands which should be originally stopbands. These unnecessary passbands can be removed by using the filter in Fig. 8 again as the band-limiting filter for the areas A, B, C and D, which completes the design.

Assume that the 2-D prototype filter $H_2(z_a, z_b)$ and the 2-D band-limiting filter $H_2'(z_a, z_b)$ are octagonally-symmetric FIR filters with $(2N_a+1)\times$

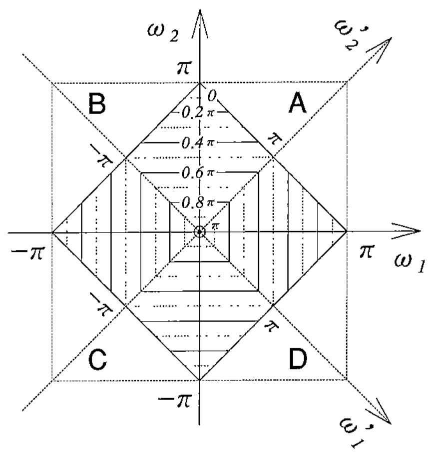

Fig. 7 Cross-sectional frequency response of band-limiting filters for BCCS with ω_3=constant. The values represent the intersections with the axis ω_3. The axes ω_1' and ω_2' are the rotated versions of ω_1 and ω_2 by Eq. (22), respectively.

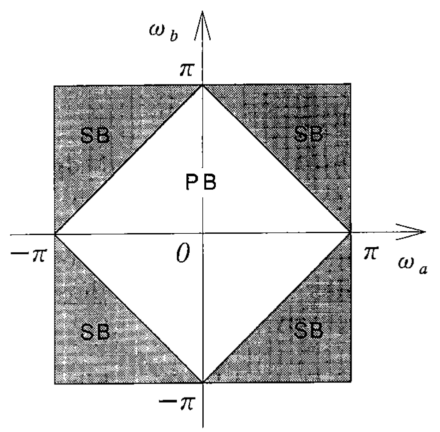

Fig. 8 2-D prototype FIR filter required for BCCS.

$(2N_b+1)$-tap and $(2N_a'+1)\times(2N_b'+1)$-tap, respectively. The transfer function of the 3-D band-limiting filter for BCCS $H_3(z_1, z_2, z_3)$ is written as

$$H_3(z_1, z_2, z_3)=H_2'(z_1, z_2)\cdot H_3'(z_1, z_2, z_3)$$
$$=\sum_{i=-N_a'}^{N_a'}\sum_{j=-N_b'}^{N_b'} h'_{ij} z_1^{-i} z_2^{-j}$$
$$\cdot\sum_{i=0}^{N_a}\sum_{j=-N_b}^{N_b} b_{ij} T_i\left(\frac{z_1z_2^{-1}+z_1^{-1}z_2+z_1z_2+z_1^{-1}z_2^{-1}}{4}\right)$$
$$\cdot z_3^{-j}, \tag{31}$$

where h'_{ij} represents the impulse response of $H_2'(z_a, z_b)$ and b_{ij}'s are constants determined from the impulse response of $H_2(z_a, z_b)$.

In this case, the resultant filter $H_3(z_1, z_2, z_3)$ is realized with two subfilters, i.e. $H_2'(z_1, z_2)$ and $H_3'(z_1, z_2, z_3)$. It should, however, be noted that the amount of hardware for such a two-stage realization is comparable with that of the case for $H_3(z_1, z_2, z_3)$ alone because the 2-D subfilter $H_2'(z_1, z_2)$ requires less amount of hardware than the 3-D subfilter $H_3'(z_1, z_2, z_3)$.

3.3.2 Considerations on an Actual Design

We first define the passband and the stopband of the 3-D filter to be designed as

$$\begin{aligned}\text{PB}=\{&(\omega_1, \omega_2, \omega_3)\,|\,|\omega_1|+|\omega_2|\leqq\omega_p^3,\\ &|\omega_2|+|\omega_3|\leqq\omega_p^3,\ |\omega_3|+|\omega_1|\leqq\omega_p^3,\\ &0\leqq|\omega_1|, |\omega_2|, |\omega_3|\leqq\pi\}\end{aligned} \tag{32}$$

$$\begin{aligned}\text{SB}=\{&(\omega_1, \omega_2, \omega_3)\,|\,|\omega_1|+|\omega_2|\geqq\omega_s^3,\\ &0\leqq|\omega_1|, |\omega_2|, |\omega_3|\leqq\pi\}\cup\\ \{&(\omega_1, \omega_2, \omega_3)\,|\,|\omega_2|+|\omega_3|\geqq\omega_s^3,\\ &0\leqq|\omega_1|, |\omega_2|, |\omega_3|\leqq\pi\}\cup\\ \{&(\omega_1, \omega_2, \omega_3)\,|\,|\omega_3|+|\omega_1|\geqq\omega_s^3,\\ &0\leqq|\omega_1|, |\omega_2|, |\omega_3|\leqq\pi\},\end{aligned} \tag{33}$$

respectively, where the positive parameters ω_p^3 and ω_s^3 determine the band-edge frequencies. For the 2-D prototype and the 2-D band-limiting filters, the passband and stopband are given as

$$\begin{aligned}\text{PB}=\{&(\omega_a, \omega_b)\,|\,|\omega_a|+|\omega_b|\leqq\omega_p^2 \text{ or } \omega_p^{2'},\\ &0\leqq|\omega_a|, |\omega_b|\leqq\pi\}\end{aligned} \tag{34}$$

$$\begin{aligned}\text{SB}=\{&(\omega_a, \omega_b)\,|\,|\omega_a|+|\omega_b|\geqq\omega_s^2 \text{ or } \omega_s^{2'},\\ &0\leqq|\omega_a|, |\omega_b|\leqq\pi\},\end{aligned} \tag{35}$$

respectively. The positive parameters ω_p^2, ω_s^2, $\omega_p^{2'}$ and $\omega_s^{2'}$ give the band-edge frequencies for the 2-D prototype and 2-D band-limiting filters, respectively.

As the 2-D band-limiting filter H_2' suppresses the unnecessary spectrum in the stopband in Eq. (33), $\omega_p^{2'}$ and $\omega_s^{2'}$ are related to ω_p^3 and ω_s^3 as

$$\omega_p^3\leqq\omega_p^{2'},\ \omega_s^{2'}\leqq\omega_s^3. \tag{36}$$

The band-edge parameters ω_p^2 and ω_s^2 for the 2-D prototype filter are determined from

$$\begin{cases}\omega_p^2\geqq\omega_p^3+0.08774\pi\\ \omega_s^2\leqq\omega_s^3-0.08774\pi,\end{cases} \tag{37}$$

which are derived by a similar consideration in Sect. 3.2.2.

Since the 3-D band-limiting filter for BCCS is composed of two subfilters, its passband and stopband deviations, δ_p^3 and δ_s^3, can be calculated from the corresponding deviations of the designed subfilters as

$$\begin{cases} \delta_p^3 = (1+\delta_p^2)(1+\delta_p^{2'}) - 1 \\ \quad \cong \delta_p^2 + \delta_p^{2'} \\ \delta_s^3 = \max\{(1+\delta_p^2)\delta_s^{2'},\ (1+\delta_p^{2'})\delta_s^2\} \\ \quad \cong \max\{\delta_s^{2'},\ \delta_s^2\}, \end{cases} \tag{38}$$

where δ_p^2, δ_s^2, $\delta_p^{2'}$ and $\delta_s^{2'}$ are the passband and the sotpband deviations of the 2-D prototype and the 2-D band-limiting filters, respectively. Thus, it is possible to minimize the deviations as well as the amount of hardware by designing the subfilters H_2 and H_2' so as to satisfy

$$\delta_s^2 = \delta_s^{2'}. \tag{39}$$

4. Realization Method for the Proposed Filters

The transfer functions designed by the proposed method can be written in the form (20). $T_i(F)$'s in Eq. (20) can be calculated recursively with the following recursion formula for Chebyshev polynomials;

$$\begin{cases} T_{i+1}(F) = 2FT_i(F) - T_{i-1}(F) \\ T_0(F) = 1 \\ T_1(F) = F, \end{cases} \tag{40}$$

which is known as "Chebyshev structure" [12]. Since Eq. (20) represents the addition of the products $T_i(F) \cdot z_3^{-j}$ weighted by b_{ij}'s, the filter can be realized as shown in Fig. 9, where F corresponds to the transformation filter. From Eq. (21), the transformation filter F is realized without multipliers. Therefore this implementation requires multipliers of order N^2 for a given filter length N. Note that the number of multipliers can be further reduced by exploiting the symmetry of coefficients. However, note also that band-limiting filters for BCCS require another set of multipliers of order N^2 for the band-limiting filter in $\omega_1-\omega_2$ frequency plane.

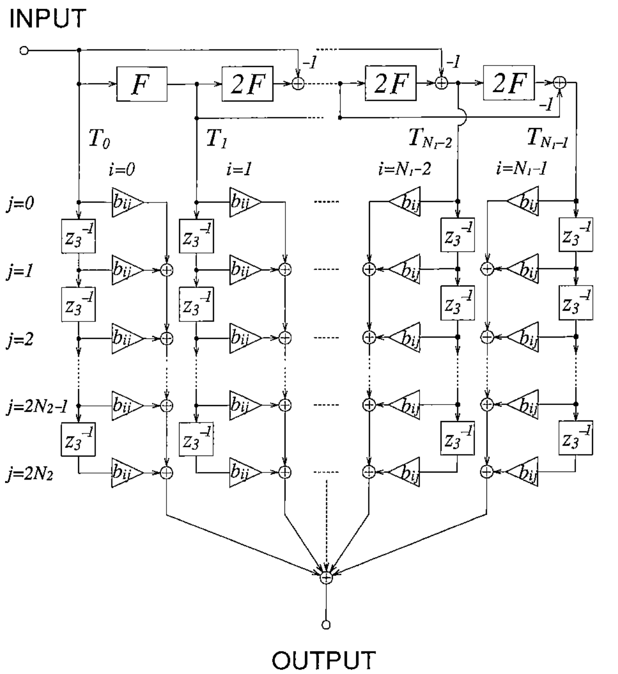

Fig. 9 Realization of the designed filter. All the notations correspond to those in Eq. (20).

The Chebyshev structure for the usual 3-D McClellan transformation requires multipliers of order N for the filter length N. Therefore, it is concluded that the proposed method makes possible the design of various types of 3-D filters which are difficult to be designed by the usual 3-D McClellan transformation, although the proposed method requires more multipliers.

5. Design Examples and Comparisons with Other Design Methods

Based on the proposed design method, this section shows two design examples of band-limiting filters for FCCS and BCCS and comparisons with other design method.

5.1 A Design Example of Band-Limiting Filters for FCCS

The design problem of band-limiting filters for FCCS is now reduced to that of the 2-D hexagonal prototype filter shown in Fig. 6. It is possible to design such a hexagonal filter as a 2-D half-band (HB) FIR filter [14]. Since the frequency response of an HB FIR filter H is symmetric with respect to $(\omega_1, \omega_2, H) = (\pi/2, \pi/2, 0.5)$, the transition band of HB FIR filter intrudes into the stopband in Fig. 6, which causes aliasing error around the boundaries of the passband and the stopband. On the other hand, an HB FIR filter has an advantage that about 50% of its impulse response coefficients are zero, which reduces the number of multipliers required in the implementation. In this section, a 3-D band-limiting filter for FCCS is designed using 2-D HB prototype filter with the following specifications;

Filter length	21×21 taps $(N_a = N_b = 10)$
Passband	$2\lvert\omega_a\rvert + \lvert\omega_b\rvert \leqq 1.340\pi$
Stopband	$2\lvert\omega_a\rvert + \lvert\omega_b\rvert \geqq 1.660\pi$
	$(0 \leqq \lvert\omega_a\rvert, \lvert\omega_b\rvert \leqq \pi)$
Weighting	$W_p : W_s = 1 : 1$.

In order to illustrate the advantage that the proposed method is applicable to rather higher-order filters, such a large number of taps is chosen in this example. The parameters ω_p^3 and ω_s^3 in Eqs. (22) and (23) are calculated from Eqs. (28) and (29) as $\omega_p^3 = 1.1645\pi$ and $\omega_s^3 = 1.8354\pi$ in this case. The prototype filter is

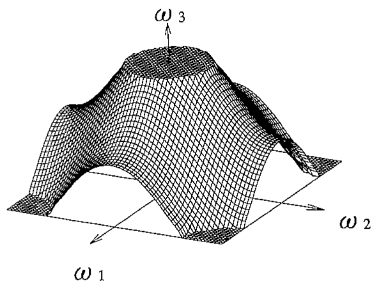

Fig. 10 -6 dB equiamplitude surface of the designed band-limiting filter for FCCS.

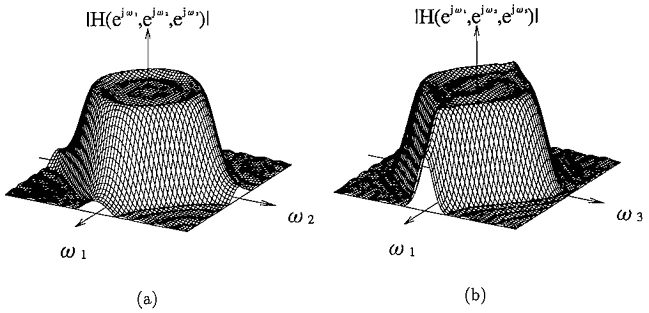

Fig. 11 Cross-sectional frequency response of the designed band-limiting filter for FCCS. (a) $\omega_3=0.6\pi$. (b) $\omega_2=0.6\pi$.

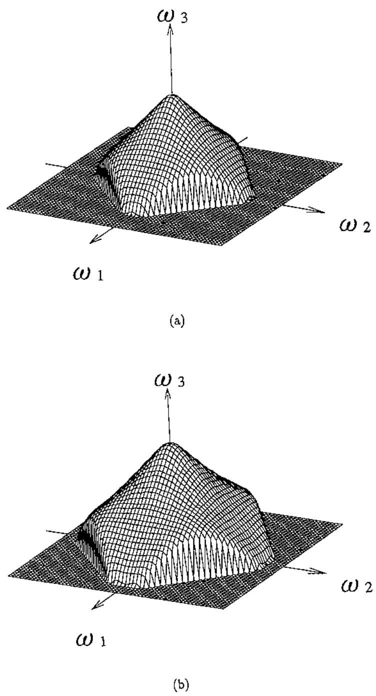

Fig. 12 Equiamplitude surfaces of the designed band-limiting filter for BCCS. (a) -3 dB. (b) -30 dB.

readily designed by the LP method [8], [9], which results in the passband and stopband deviation 0.0275 with 3708 sampling points taken in the frequency domain. An application of the McClellan transformation (21) to the designed prototype filter completes the design procedure. Figure 10 shows the -6 dB equiamplitude surface of the designed 3-D band-limiting filter, where only the space $\omega_3>0$ is shown. The cross-sectional 2-D responses with $\omega_3=0.6\pi$ and $\omega_2=0.6\pi$ are also shown in Fig. 11. From these figures, it is observed that the proposed design method well approximates the ideal response in Fig. 2 (b).

5. 2 A Design Example of Band-Limiting Filters for BCCS

In this example, a 3-D band-limiting filter for BCCS is designed with $\omega_p^3=0.600\pi$ and $\omega_s^3=1.000\pi$ in Eqs. (32) and (33). The specifications of the 2-D prototype filter and the 2-D band-limiting filter are given as

Filter Length	21×21 taps ($N_a=N_b=10$)
Passband	$\lvert\omega_a\rvert+\lvert\omega_b\rvert\leqq0.6877\pi$
Stopband	$\lvert\omega_a\rvert+\lvert\omega_b\rvert\geqq0.9123\pi$
	$(0\leqq\lvert\omega_a\rvert, \lvert\omega_b\rvert\leqq\pi)$
Weighting	$W_p:W_s=1:0.7$

and

Filter Length	13×13 taps ($N_a'=N_b'=6$)
Passband	$\lvert\omega_a\rvert+\lvert\omega_b\rvert\leqq0.600\pi$
Stopband	$\lvert\omega_a\rvert+\lvert\omega_b\rvert\geqq1.000\pi$
	$(0\leqq\lvert\omega_a\rvert, \lvert\omega_b\rvert\leqq\pi)$
Weighting	$W_p:W_s=1:0.4$,

respectively. Note that the weightings are chosen to satisfy Eq. (39) approximately. The LP technique is again employed for the design of these filters. $\delta_p^2=0.0154$ and $\delta_s^2=0.0222$ are obtained with 3748 sampling points for the 2-D prototype filter, and $\delta_p^{2'}=0.00919$ and $\delta_s^{2'}=0.0231$ with 3748 sampling points for the 2-D prototype filter, from which the resultant deviations are calculated as $\delta_p^3=0.0247$ and $\delta_s^3=0.0234$.

Figure 12 gives the -3 dB and -30 dB equiamplitude surfaces of the designed band-limiting filter. In view of these figures, fairly good characteristics can be obtained with the proposed method.

5. 3 Comparison with Other Design Methods

To verify the advantage of the proposed method, the same band-limiting filter for BCCS is designed by other methods, Method 1 and Method 2, which use 2-D prototype FIR filters. First these two methods are outlined.

Method 1 is a revised version of the design method in Ref. [15]. The following procedure summarizes the Method 1 specific to the design of 3-D band-limiting filters for BCCS.

1. Read the filter length N and the parameters ω_p^3 and ω_s^3 in Eqs. (32) and (33).
2. Calculate the cross-sectional ideal frequency responses $H_c(\omega_1, \omega_2)(k)$ in Eqs. (32) and (33) for $\omega_3 = 2\pi k/N\,(0 \leqq k \leqq (N-1)/2)$.
3. Design 2-D $N \times N$-tap octagonally-symmetric FIR filters (impulse response: $h_{ij}(k)$) for $H_c(\omega_1, \omega_2)(k)\,(0 \leqq k \leqq (N-1)/2)$ by the LP method.
4. Compute the 1-D discrete Fourier transform of $h_{ij}(k)$ with respect to k to obtain the desired impulse response h_{ijk}.

On the other hand, Eqs. (32) and (33) imply that the 3-D band-limiting filter for BCCS can be approximated by multiplying three diamond-shaped filters in ω_1-ω_2, ω_2-ω_3 and ω_1-ω_3 planes. Method 2 designs the 3-D band-limiting filter for BCCS based on this property. The design procedure is summarized as follows;

1. Read the filter length N and the parameters ω_p^3 and ω_s^3 in Eqs. (32) and (33).
2. Design a 2-D $(N+1)/2 \times (N+1)/2$-tap octagonally-symmetric FIR filter $H_2(e^{j\omega_1}, e^{j\omega_2})$ for Eqs. (34) and (35) with $\omega_p^2 = \omega_p^3$, $\omega_s^2 = \omega_s^3$ and $W_p : W_s = 3:1$.
3. Cascade the three filters $H_2(e^{j\omega_1}, e^{j\omega_2})$, $H_2(e^{j\omega_2}, e^{j\omega_3})$ and $H_2(e^{j\omega_1}, e^{j\omega_3})$ to obtain the desired filter.

By using these two methods, the 3-D band-limiting filters for BCCS have been designed. The results are summarized in Table 1, where the band-edge parameters ω_p^3 and ω_s^3, the filter length, the number of independent multipliers N_{ADD} and the passband and stopband deviations δ_p^3 and δ_s^3 are listed for each filter. As can be seen from Table 1, the proposed design method attains the lowest deviations. Method 1 gives the poorest results although it tequires the largest number of multipliers. To avoid a large error arround band edges, the passband and stopband deviations are again calculated in the region Eqs. (32) and (33) with $\omega_p^3 = 0.57\pi$ and $\omega_s^3 = 1.03\pi$, and are shown as $\delta_p^{3'}$ and $\delta_s^{3'}$ in Table 1, respectively. Such large deviations come from the error in Fourier series decomposition and cannot be reduced without increasing the filter length in the direction of n_3. On the other hand, Method 2 requires less multipliers, but a relatively large number of taps are needed to obtain comparable results. In 3-D filtering, a reduction of the number of frame memories is very important. The advantage of the proposed method is now verified from such a point of view.

Table 1 Comparisons of the filters designed by the proposed method, Method 1 and Method 2.

	Proposed Method	Method 1	Method 2
ω_p^3	0.60π	0.60π	0.60π
ω_s^3	1.00π	1.00π	1.00π
Filter length	21 × 21 × 21	21 × 21 × 21	25 × 25 × 25
N_{ADD}	94	726	84
δ_p^3	0.0247	0.132	0.0254
δ_s^3	0.0231	0.111	0.0254
$\delta_p^{3'}$	——	0.0911	——
$\delta_s^{3'}$	——	0.104	——

6. Concluding Remarks

This paper has proposed a new design method of 3-D band-limiting filters for face-centered cubic sampling (FCCS) and body-centered cubic sampling (BCCS). This method employs the 2-D McClellan transformation and 2-D prototype filters to obtain 3-D filters. 3-D filters with more than 20 taps can be easily designed with good characteristics, which is observed by the design examples given in this paper. The effective implementation of the proposed filter is also considered.

As shown in Sect. 2, various types of alias-free basebands other than the first Brillouin zone exist. As far as a given baseband shape satisfies the condition in Sect. 3. 1, the band-limiting filter can be designed with the proposed method. Such a design is left for future work.

References

[1] Dudgeon, D. E. and Mersereau, R. M., *Multidimensional Digital Signal Processing*, Prentice-Hall, New Jersey, 1984.

[2] Dubois, E., "The Sampling and Reconstruction of Time-Varying Imagery with Application in Video Systems," *Proc. IEEE*, vol. 73, no. 4, pp. 502–522, Apr. 1985.

[3] Tonge, G. J., "The Sampling of Television Images," *Experimental & Development Rep. 112/81*, Independent Broadcasting Authority, May 1981.

[4] Tonge, G. J., "Three-Dimensional Filters for Television Sampling," *Experimental & Development Rep. 117/82*, Independent Broadcasting Authority, Jun. 1982.

[5] Schamel, G., "Pre-and Postfiltering of HDTV Signals for Sampling Rate Reduction and Display Up-Conversion," *IEEE Trans. Circuits & Syst.*, vol. CAS-34, no. 11, pp. 1432–1439, Nov. 1987.

[6] Kagoshima, T., Kawamata, M. and Higuchi, T., "Design of Parallel Separable 3-D Digital Filters and Its Application to Video Signal Processing," *Proc. 7th Digital Signal Processing Symp.*, pp. 139–144, Nov. 1992.

[7] Fukinuki, T., *Multi-Dimensional TV Signal Processing*, Nikkan-Kogyo-Shimbunsha, Tokyo, 1987.

[8] Hu, J. V. and Rabiner, L. R., "Design Techniques for Two-Dimensional Digital Filters," *IEEE Trans. Audio Electroacoust.*, vol. AU-20, no. 4, pp. 249–257, Dec. 1972.

[9] Higuchi, T., Ohki, M. and Kawamata, M., "Optimal Design of Three-Dimensional FIR Digital Filters — Design Method by Linear Programming and Reduction of Computations by Exploiting Symmetries," *Trans. IEICE*, vol. J70-A, no. 7, pp. 1042–1050, Jul. 1987.

[10] McClellan, J. H., "The Design of Two-dimensional Digital Filters by Transformations," *Proc. the 7th Annu. Princeton Conf. Inf. Sci. and Syst.*, pp. 247–251, 1973.

[11] Mersereau, R. M., Mecklenbraüker, W. F. G. and Quatieri, Jr., T. F., "McClellan Transformation for 2-D

Digital Filtering: I-Design," *IEEE Trans. Circuits & Syst.*, vol. CAS-23, no. 7, pp. 405–414, Jul. 1976.

[12] McClellan, J. H. and Chan D. S. K., "A 2-D FIR Filter Structure Derived from the Chebyshev Recursion," *IEEE Trans. Circuits & Syst.*, vol. CAS-24, no. 7, pp. 372–378, Jul. 1977.

[13] Kondo, K., Sugii, Y. and Hamada, N., "A Design of Digital Filter to Detect the Planar Signal Having Particular Direction," *1989 IEICE Spring Nat. Conv. Record*, A-315, pp. 1–318, Mar. 1989.

[14] Yoshida, T., Nishihara, A. and Fujii, N., "A Design Method of 2-D Maximally Flat Diamond-Shaped Half-Band FIR Filters," *Trans. IEICE*, vol. E73, no. 6, pp. 901–907, Jun. 1990.

[15] Zervakis, M. E. and Venetsanopoulos, A. N., "Design of Three-Dimensional Digital Filters Using Two-Dimensional Rotated Filters," *IEEE Trans. Circuits & Syst.*, vol. CAS-34, no. 12, pp. 1452–1469, Dec. 1987.

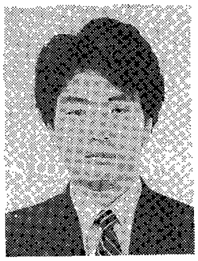

Toshiyuki Yoshida was born in Fukui, Japan on September 11, 1963. He received B.E., M.E., and D.E. degrees all in electronics from Tokyo Institute of Technology in 1986, 1988 and 1991, respectively. He is presently a research associate in the Department of Physical Electronics, Faculty of Engineering, Tokyo Institute of Technology. His main research interests are in the area of multi-dimensional digital signal processing and filter design.

Akinori Nishihara was born in Fukuoka, Japan on February 26, 1951. He received B.E., M.E. and Dr.Eng. degrees in Electronics from Tokyo Institute of Technology in 1973, 1975 and 1978, respectively. Since 1978 he has been with Tokyo Institute of Technology, where he is now Associate Professor of Department of Physical Electronics, Faculty of Engineering. He is responsible for education and research in the field of circuits and systems. His main research interests are in analog and digital filter design, hardware and software of digital signal processors. He received Young Engineer award from IEICE in 1982. Dr. Nishihara is a member of IEEE.

Nobuo Fujii received a B.E. degree from Keio University, Yokohama, Japan, and M.E. and Doctor of Engineering degrees from Tokyo Institute of Technology, Tokyo, Japan, in 1966, 1968, and 1971, respectively. Since 1971, he has been with the Faculty of Engineering, Tokyo Institute of Technology where he is now a professor in the department of Physical Electronics. From 1984 to 1985, he was a visiting Scholar at the University of California Santa Barbara. His main interest lies in the field of active network theory and analog integrated circuits. He is the recipient of the 1983 Best Paper Award of the Institution of Electrical and Communication Engineers of Japan. He is the author of 5 books. Dr. Fujii is a member of the Institution of Electrical and Electronics Engineers and the Institution of Electrical Engineers of Japan.